Phase Behavior and Molecular Mobility in Polyurethane/Styrene–Acrylonitrile Blends

A. S. VATALIS,[1] A. KANAPITSAS,[2] C. G. DELIDES,[1] K. VIRAS,[3] P. PISSIS[2]

[1] Laboratories of Physics and Materials Technology, Technological Educational Institute (TEI) of Kozani, 50100 Kila, Kozani, Greece

[2] Physics Department, National Technical University of Athens, Zografou Campus, 15780 Athens, Greece

[3] Department of Chemistry, Physical Chemistry Laboratory, National and Kapodistrian University of Athens, Panepistimioupolis, 15771 Athens, Greece

Received 14 March 2000; accepted 12 August 2000

ABSTRACT: Differential scanning calorimetry (DSC), thermally stimulated depolarization currents (TSDC) techniques, dielectric relaxation spectroscopy (DRS), and dynamic mechanical thermal analysis (DMTA), covering together a wide range of temperatures and frequencies, were employed to investigate molecular mobility and microphase separation in blends of crosslinked polyurethane (PUR) and styrene–acrylonitrile (SAN) copolymer, prepared by reactive blending with polymer polyols. The results by each technique indicate that the degree of microphase separation of PUR into hard-segment (HS) microdomains and soft-segment (SS) microphase increases on addition of SAN. The various techniques were critically compared to each other, with respect to their characteristic time and length scales, on the basis of activation diagrams (Arrhenius plots). The results show that for the dynamic glass transition of the PUR SS microphase the characteristic time scales at the same temperature are similar for DMTA, DSC, and TSDC and shorter for DRS. In terms of fragility, the PUR/SAN blends are classified as fragile systems. © 2001 John Wiley & Sons, Inc. J Appl Polym Sci 80: 1071–1084, 2001

Key words: polymer blends; crosslinked polyurethanes; styrene–acrylonitrile copolymer; microphase separation; dynamic glass transition

INTRODUCTION

Segmented polyurethanes (SPUs), characterized by microphase-separated morphology, arising from the incompatibility of hard segments (HS) and soft segments (SS),[1] are often used in multicomponent polymeric systems, such as polymer mixtures, blends, and interpenetrating polymer networks. These multicomponent systems provide the possibility to combine the versatile properties of SPUs with other, often contrary, properties of the other components. Very often the second component is a thermoplastic hard polymer to improve the mechanical properties of the multicomponent system.[2,3] Specific physical and chemical interactions in such systems may result in a modification of the degree of microphase separation (DMS) of SPUs into microdomains rich in HS (HS microdomains) and a microphase rich in SS (SS microphase).[2,4]

Correspondence to: P. Pissis (ppissis@central.ntua.gr).

Journal of Applied Polymer Science, Vol. 80, 1071–1084 (2001)

In this work we study structure–property relationships in blends of crosslinked polyurethanes (PURs) and styrene–acrylonitrile (SAN) copolymer. The PURs are based on polyoxypropylene glycol with 15 wt % ethylene oxide termination, with average molecular weight 3500 and functionality 2.8. The ratio of acrylonitrile and styrene in SAN is 50/50. The method of reactive blending was employed for the PUR formation with polymer polyols.[2]

Various experimental techniques were used by several investigators to study phase behavior and molecular mobility in multicomponent polymeric systems, in which each technique was characterized by its own time and length scales.[5,6] In general different techniques probe the mobility of units of different size and a particular mechanism of molecular mobility may be active or not with respect to a technique.

Time scales, typically determined by heating rate and/or frequency of measurements, can be modified externally, at least partly. Length scales are more subtle. A particular difficulty there arises from the fact that very often in multicomponent polymeric systems we are interested in glass transitions and the investigation of primary (main) relaxations associated with the glass transition (dynamic glass transition), to get information on morphology and microphase separation. However, the glass transition has its own characteristic length scale.[7] The relation of that length scale to the characteristic length scale of the experimental technique used is significant for the interpretation of the experimental results. Thus, it is not surprising that the relationships between the various experimental techniques are not always clear and that this subject has attracted much interest in recent years.[8–11]

Here various experimental techniques are employed to investigate structure–property relationships in PUR/SAN blends: differential scanning calorimetry (DSC), thermally stimulated depolarization currents (TSDC) techniques, dielectric relaxation spectroscopy (DRS), and dynamic mechanical thermal analysis (DMTA). From the methodological point of view one area of concern here is to critically discuss the results obtained by the various techniques in relation to each other, in an attempt to contribute to a better understanding of the relationships between the various techniques.[8–11]

EXPERIMENTAL

Materials

The polymer polyols were synthesized from polyoxypropylene glycol (PPG) with 15 wt % ethylene oxide termination, having an average molecular weight of 3500 and a functionality of 2.8, and styrene–acrylonitrile (SAN) copolymer whose composition ratio was 50/50 acrylonitrile/styrene. PUR/SAN and PUR were prepared from the polymer polyol (or polyol itself), 4.4 diphenylmethane diisocyanate (MDI), and 1,4 butandiol (BDO) in the equivalent ratio polyol/BDO/MDI = 1/1/2 (2.5% excess of MDI). The samples were prepared by the one-shot technique at 110°C and stored at that temperature for 24 h. The SAN copolymer content in the samples was, respectively, 0, 10, and 20%. Details of the preparation of the samples are given elsewhere.[2]

Methods

Differential scanning calorimetry (DSC) measurements were carried out using a Perkin–Elmer DSC4 differential scanning calorimeter (Perkin–Elmer, Foster City, CA) at heating scans from −120 to 30°C and from 20 to 250°C with a heating rate of 10°C/min.

The thermally stimulated depolarization currents (TSDC) method consists of measuring the thermally activated release of frozen-in polarization and corresponds to measuring dielectric losses versus temperature at low frequencies in the range of 10^{-4} to 10^{-2} Hz.[12] By this method the sample is inserted between the plates of a capacitor, made of brass, polarized by the application of a dc field E and cooled down to liquid nitrogen temperature to freeze in the polarization. The sample is then short-circuited and reheated at a constant rate b. A discharge current is generated as a function of temperature, which is measured with a sensitive electrometer (Keithley 610C; Keithley Metrabyte, Taunton, MA). The TSDC spectrum thus obtained consists of several peaks whose shape and location are characteristic of the relaxation mechanisms of the sample. The analysis of the shape and the location of a TSDC peak makes it possible to obtain the activation energy W, the preexponential factor τ_o in the Arrhenius equation, and the contribution $\Delta\epsilon$ of the peak to the static permittivity. A common experimental apparatus for TSDC measurements was used in the temperature range from −180 to 30°C.[13]

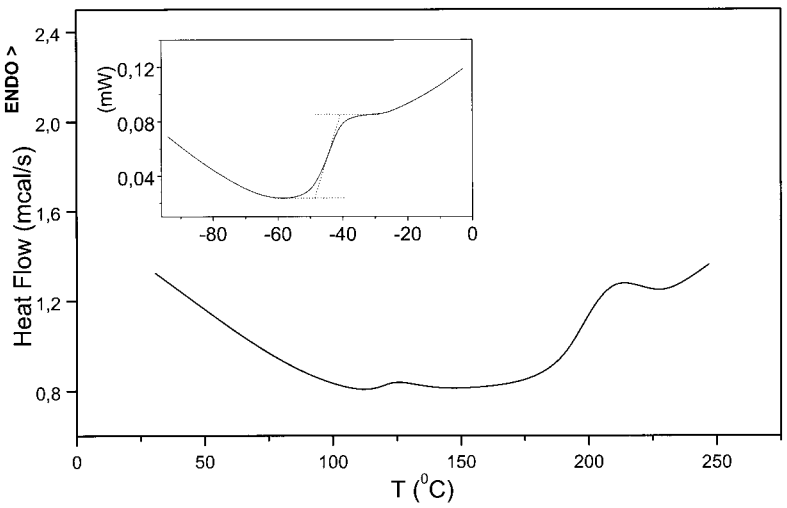

Figure 1 DSC thermogram (heat flow versus temperature) for the sample PUR/20%SAN in the temperature range 30–250°C. The inset shows the DSC thermogram for the same sample in the region of T_g of PUR and the determination of T_g (midpoint value).

Broadband dielectric relaxation spectroscopy (DRS) measurements (two-terminal complex admittance measurements) were taken using a Schlumberger frequency response analyzer (FRA 1260, Farnborough, Hampshire, UK) supplemented by a buffer amplifier of variable gain (10^{-2}–10^6 Hz). The sample (of cylindrical shape of 20-mm diameter and 1.5-mm thickness, similar to TSDC measurements) was sandwiched between two gold-plated stainless steel electrodes. The temperature was controlled by a custom-made nitrogen gas jet heating system covering a broad temperature range from −120 to 30°C with a resolution of ±0.02°C.

For dynamic mechanical thermal analysis (DMTA) measurements in bending mode a Polymer Laboratories (Loughborough, UK) apparatus (Model PL-MK II) was used at the frequencies of 0.1, 1, 10, and 100 Hz from −100 to 200°C.

RESULTS

Differential Scanning Calorimetry

Figure 1 shows DSC plots for the blend with 20% SAN (PUR/20%SAN). At subzero temperatures the glass transition of the microphase rich in soft segments (SS microphase) of PUR was recorded. The midpoint glass-transition temperature T_g was determined to be $T_g = -44$°C and the specific heat increment at T_g, $\Delta C_p = 0.40$ J/g deg^{-1}. At higher temperatures the glass transition of the SAN component was observed and T_g was determined to be $T_g = 118$°C. This glass transition is not observed in pure PUR. The endothermic peak at about 210°C, observed also in the pure PUR sample, is associated with softening of the microdomains rich in hard segments (HS microdomains).[14] It shifts slightly from 215°C in PUR to 210°C in PUR/20%SAN.

T_g of the SS microphase (midpoint values throughout this work) is plotted in Figure 2 as a function of SAN content. The corresponding specific heat increment ΔC_p is plotted in Figure 3. As expected, ΔC_p decreases with increasing SAN content. Interestingly, the decrease of ΔC_p is larger than the decrease in the PUR component. T_g increases slightly with increasing SAN content (Fig. 2). On the other hand, for the glass transition attributed to the SAN component the same value of T_g, 118°C, was measured for both PUR/10%SAN and PUR/20%SAN, whereas ΔC_p was found to increase with increasing SAN content.

Thermally Stimulated Depolarization Currents (TSDC) Measurements

Figure 4 shows a typical TSDC thermogram measured on PUR/10%SAN at a heating rate $b = 3$°C/min. Similar thermograms were also obtained with PUR and PUR/20%SAN. Four dispersions are observed in the thermograms. Those at low temperatures are attributed to secondary γ and β

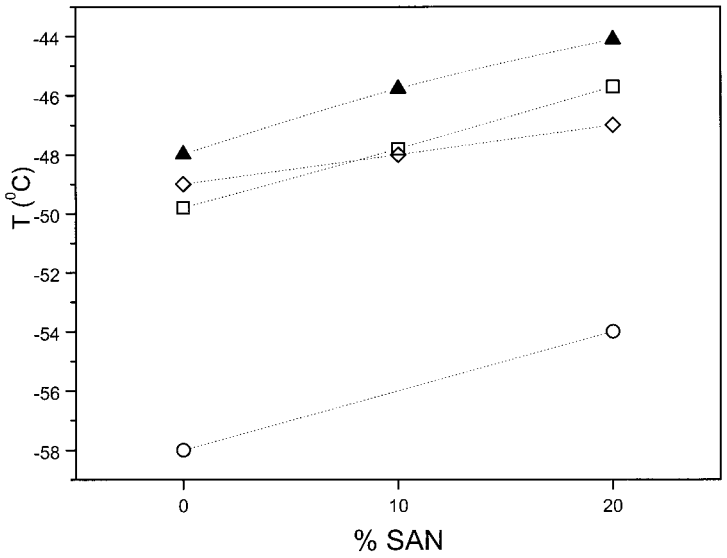

Figure 2 Glass-transition temperatures of PUR versus SAN content determined by DSC (T_g, ▲), TSDC (T_α, ◇), DRS ($T_{g\ diel}$, ○), and DMTA ($T_{g\ mech}$, □). The lines are to guide the eye.

relaxations of PUR in the order of increasing temperature (−160 and −120°C in Fig. 4). The peaks at high temperatures have been attributed in several polyurethane systems to the dipolar α relaxation associated with the glass transition of the SS microphase and to interfacial Maxwell–Wagner–Sillars (MWS) polarization at the interfaces between HS microdomains and SS microphase.[3,15,16]

No systematic variation with SAN content was observed for the temperature position of the secondary γ and β relaxations. The α peak and the MWS peak were found to systematically shift to higher temperatures with increasing SAN content: the α peak from −49°C for PUR to −47°C for PUR/20%SAN (Fig. 2) and the MWS peak from −15°C for PUR to −6°C for PUR/20%SAN (Fig. 5).

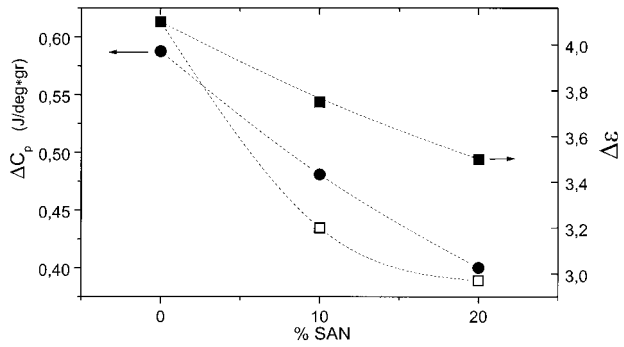

Figure 3 Specific heat increment ΔC_p at T_g of PUR (●) and dielectric relaxation strength $\Delta\epsilon$ of the corresponding TSDC α peak (■). The open squares give the normalized magnitude I_α of the TSDC α peak (in arbitrary units, scaled with $\Delta\epsilon$ at 0% SAN). The lines are to guide the eye.

The contribution $\Delta\epsilon$ of a TSDC peak to the static permittivity is given by[12]

$$\Delta\varepsilon = \frac{Q}{A\varepsilon_0 E_p} = \frac{\int I\,dt}{A\varepsilon_0 E_p} \tag{1}$$

where Q is the depolarization charge, obtained from the surface area of the peak; A is the cross-sectional area of the sample; E_p is the polarizing field; and ϵ_0 the permittivity of free space. For the α relaxation $\Delta\epsilon$ was found to systematically decrease with increasing SAN content from 4.1 for PUR to 3.5 for PUR/20%SAN, that is, less than proportional to the decrease of the PUR component (Fig. 3). The normalized magnitude of the α peak I_α (normalized to the same polarizing field and the same heating rate) has also been plotted in Figure 3. It decreases faster than $\Delta\epsilon$ with increasing SAN content, which results from the fact that the α peak is broader in the blends (full half-width 15.5°C in PUR and 17.0°C in the blends), suggesting a broader distribution of relaxation times in the blends.[12,13] Thus, one has to be careful, when considering the normalized magnitude of a TSDC peak as a measure of the num-

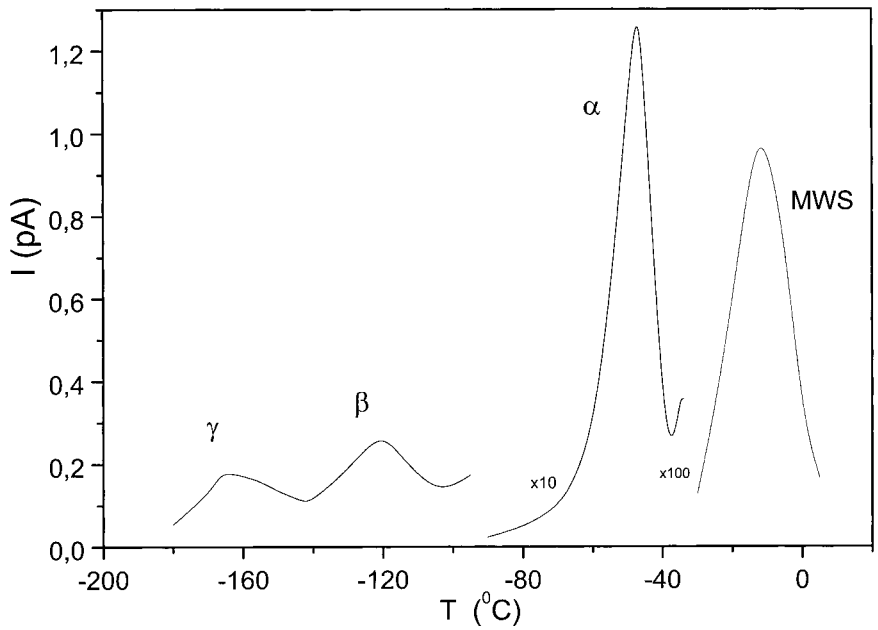

Figure 4 TSDC thermogram of PUR/10%SAN measured at a heating rate of 3°C/min.

ber of relaxing units contributing to the peak,[12,13] that there is no change in the shape of the peak.

For the MWS peak $\Delta\epsilon$ increases significantly with increasing SAN content (Fig. 5), suggesting (together with the shift of the peak to higher temperatures) a change in the microphase-separated morphology of the samples.[15] The increase is less significant in the normalized peak magnitude I_{MWS} (Fig. 5), in agreement with the full half-width of the peak increasing from 21.0°C in PUR to 28.5°C in PUR/10%SAN and to 31.0°C in PUR/20%SAN.

Dielectric Relaxation Spectroscopy (DRS)

Figure 6 shows the dielectric losses ϵ'' (the imaginary part of dielectric permittivity, $\epsilon = \epsilon' - i\epsilon''$)

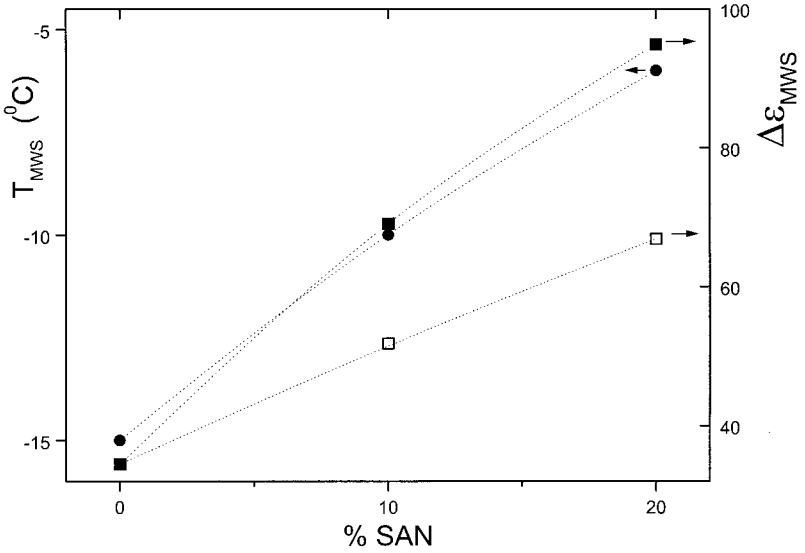

Figure 5 Peak temperature T_{MWS} (●) and dielectric strength $\Delta\epsilon_{MWS}$ (■) of the TSDC MWS peak versus SAN content. The open squares give the normalized magnitude I_{MWS} of the TSDC MWS peak (in arbitrary units, scaled with $\Delta\epsilon_{MWS}$ at 0% SAN). The lines are to guide the eye.

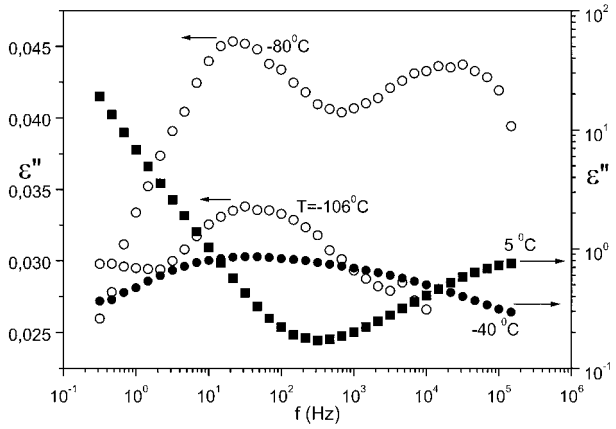

Figure 6 Dielectric losses ϵ'' versus frequency f for PUR at several temperatures indicated on the plot. Values of ϵ'' at -40 and 5°C (filled symbols) are given in a logarithmic scale.

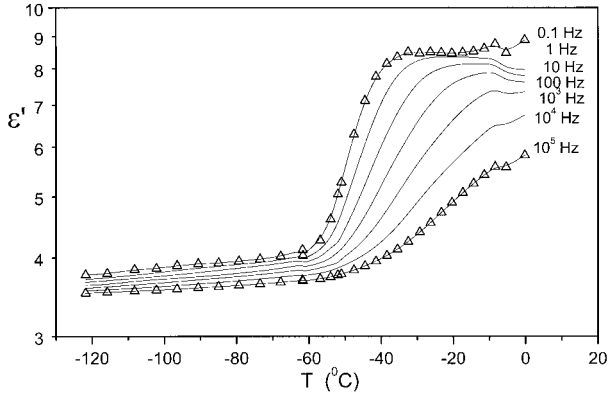

Figure 7 Isochronal plots of $\epsilon'(T)$ for PUR/20%SAN at several frequencies indicated on the plot. For 0.1 and 10^5 Hz data and lines to guide the eyes are shown; otherwise, only guide lines are shown.

against frequency f for PUR at several temperatures indicated on the plot. All the relaxation mechanisms exhibited by PUR are shown in this plot. At -106°C the γ relaxation is observed centered at about 25 Hz. At higher temperature, -80°C, the loss peak has been shifted to the right (at about 20 kHz), whereas the slower β relaxation has entered the frequency window of measurements (at about 20 Hz). The α relaxation associated with the glass transition of the SS microphase enters the frequency window of measurements at temperatures higher than T_g (broad and asymmetric peak at -40°C, logarithmic scale for ϵ''). Finally, at 5°C the behavior is dominated by dc conductivity giving rise to high values of ϵ'' at low frequencies.

To compare the results of DRS measurements with those of the nonisothermal DSC and TSDC techniques (and DMTA, to be shown later), Figure 7 shows isochronal (constant frequency) plots of the real part ϵ' of dielectric permittivity against temperature for PUR/20%SAN at several frequencies indicated on the plot. The plot is dominated by the step in the region of the glass transition of the SS PUR microphase shifting to higher temperatures and becoming more flat with increasing frequency. $\Delta\epsilon$, determined from the height of the step at the lowest frequency of 0.1 Hz, decreases with SAN content from 5.1 for PUR to 4.5 for PUR/20%SAN, in rather good agreement with the TSDC data (Fig. 3), considering that $\Delta\epsilon$ is temperature dependent.[17–19]

Figure 8 shows $\epsilon''(T)$ plots at $f = 0.1$ Hz for PUR and PUR/20%SAN. The β relaxation is observed at about -95°C (the γ relaxation is at lower temperatures, out of the range of measurements), the α relaxation at about -50°C, and dc conductivity at higher temperatures. Compared to PUR, the plot for PUR/20%SAN shows no significant changes for the β relaxation, a shift of the α relaxation to higher temperatures (in agreement with DSC and TSDC results), and lower contribution of dc conductivity.

Dynamic Mechanical Thermal Analysis (DMTA)

Figure 9 shows results of DMTA measurements, shear modulus G', and shear loss tangent tan δ, for PUR/20%SAN at 100 Hz. At this frequency T_g, determined as the loss peak temperature, is -21°C for PUR and 139°C for SAN. Both T_g's shift to lower temperatures with decreasing frequency of measurements, a point that is discussed

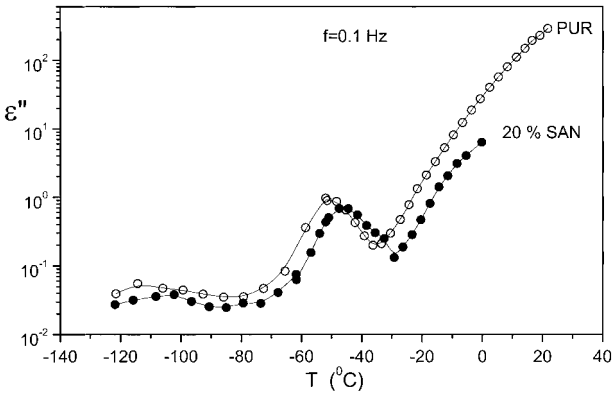

Figure 8 $\epsilon''(T)$ spectra at $f = 0.1$ Hz for PUR and PUR/20%SAN.

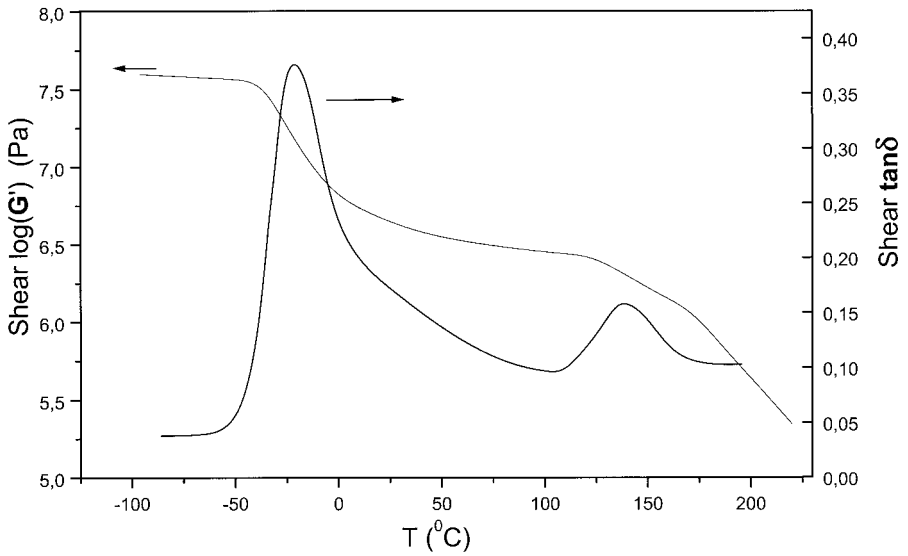

Figure 9 Real part of shear modulus G' and loss tangent tan δ versus temperature at f = 100 Hz for PUR/20%SAN.

later. In contrast to DSC, DMTA shows a slight decrease of T_g of SAN with increasing PUR content, T_g = 139°C for PUR/20%SAN and T_g = 137°C for PUR/10%SAN, both at 100 Hz. Results obtained with different blend compositions show an improvement of mechanical properties on addition of SAN: a plateau in G' is observed between the two T_g's (rubberlike behavior[2]), where the plateau value increases with increasing SAN content. At temperatures higher than about 180°C, G' decreases significantly, in correlation with softening and melting of the HS microdomains of PUR observed by DSC (Fig. 1).

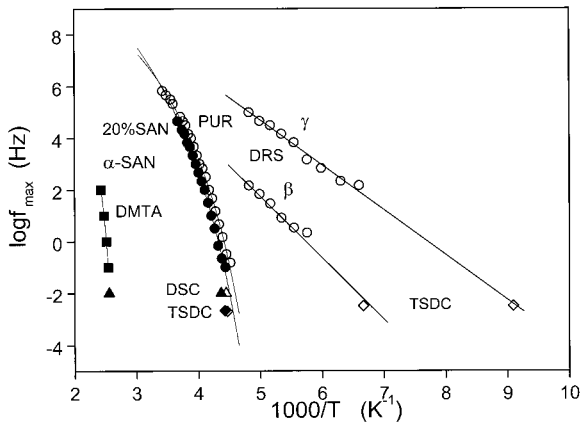

Figure 10 Arrhenius plot for the dielectric α, β, and γ relaxations in PUR (○), for the dielectric α relaxation of PUR in PUR/20%SAN (●) and for the mechanical α relaxation of SAN in PUR/20%SAN (■). The lines are fittings of the VTHF eq. (5) for α. Included are TSDC peak temperatures (◇, ◆) at the equivalent frequency of 1.6 mHz and DSC T_g's (△, ▲) at the equivalent frequency of 10 mHz.

DISCUSSION

The dynamics of the different relaxation processes active in the blends under investigation is best discussed on the basis of Arrhenius plots (activation diagrams). The plot in Figure 10 contains DRS data for the secondary γ and β relaxations in PUR and for the primary α relaxation of the PUR SS microphase in PUR and in PUR/20%SAN, as well as DMTA data for the α relaxation of SAN in PUR/20%SAN. For these techniques f_{max} in Figure 10 is the frequency of the corresponding loss peak. For comparison, TSDC and DSC data have been included in the plot.

The coordinates of the TSDC points in Figure 10 are given by the peak temperature T_m of the corresponding TSDC peak and the equivalent frequency of 1.6 mHz. The latter corresponds to a dielectric relaxation time of τ = 100 s, in agreement with experimental results showing that in many systems $\tau(T_m)$ is in the range of 100 s.[12,13] The coordinates of the DSC points in Figure 10 are given by T_g determined by DSC and the equivalent frequency of T_g (DSC) obtained from eq. (7):

$$f_{eq} = \frac{b}{2\pi\alpha\delta T} \tag{2}$$

Table I Fitting Parameters of Eqs. (4), (5), and (8) to the Data in Figs. 10 and 11 for PUR, PUR/10%SAN, and PUR/20%SAN

			Eq. (4)				α-Relaxation					
			γ-Relaxation		β-Relaxation		Eq. (5)			Eq. (8)		
Sample	Technique	Component	E (eV)	f_0 (s)	E (eV)	f_0 (s)	log A	B (K)	T_0 (K)	log A	D	T_0 (K)
PUR	DRS	PUR	0.34	2.6×10^{11}	0.37	2.3×10^{10}	11.4	678	167	11.4	4.1	167
PUR/20%SAN	DRS	PUR					12.7	877	162	12.7	5.4	162
PUR	DMTA	PUR					19.6	1948	137	19.6	14.2	137
PUR/10%SAN	DMTA	PUR					18.7	1836	142	18.7	12.9	142
PUR/20%SAN	DMTA	PUR					15.9	1353	152	15.9	8.9	152
PUR/10%SAN	DMTA	SAN					11.9	791	330	11.9	5.5	330
PUR/20%SAN	DMTA	SAN					13.2	1135	366	13.2	3.1	366

In this equation b is the cooling rate (10°C/min, equal to the heating rate), α is a constant of the order 1, and δT is the mean temperature fluctuation (of the order of 2°C[20]). It follows that f_{eq} = 10 mHz. Another equation to transform cooling rates into frequencies, proposed exclusively for poly(vinyl acetate),[21]

$$f_{eq} = \frac{b}{2\pi 15K} \tag{3}$$

would here give f_{eq} = 1.8 mHz.

The Arrhenius equation

$$f_{\max} = f_0 \exp\left(-\frac{E}{kT}\right) \tag{4}$$

where f_0 is a constant, E is the activation energy, and k is Boltzmann's constant, gives good fits to the secondary β and γ relaxations in Figure 10. The fitting parameters are listed in Table I. They take values typical for local, secondary relaxations in this temperature region and are similar to those determined for other polyurethane systems.[3,16–18] Within the limits of experimental errors, similar values were obtained for PUR/20%SAN. Bearing in mind the need for extrapolation, the TSDC data for the γ and β relaxations in Figure 10 are in rather good agreement with the DRS data, providing support that both the DRS loss peaks and the TSDC peaks refer to the same mechanism. The γ relaxation in polyurethane systems has been associated with local motion of $(CH_2)_n$ sequences.[3,16–18,22] The β relaxation has been attributed to the motion of the polar carbonyl groups with attached water molecules.[3,16–18,22]

The data for the α relaxation of the PUR SS microphase are shown in more detail in Figure 11. Mechanical α relaxation data of the PUR SS microphase have been added to the dielectric ones. Both the dielectric and the mechanical data in Figure 11 show that at each temperature the α relaxation of the PUR SS microphase becomes slower in the blends. The TSDC and DSC data show the same trend: for the same equivalent frequency the characteristic temperatures are larger in the blends. For the same sample at each temperature the dielectric relaxation is faster than the mechanical one. The data for the dielectric and mechanical α relaxations in Figures 10 and 11 have been well fitted by the characteristic for the glass-transition Vogel–Tammann–Fulcher–Hesse (VTFH) equation[7,23]

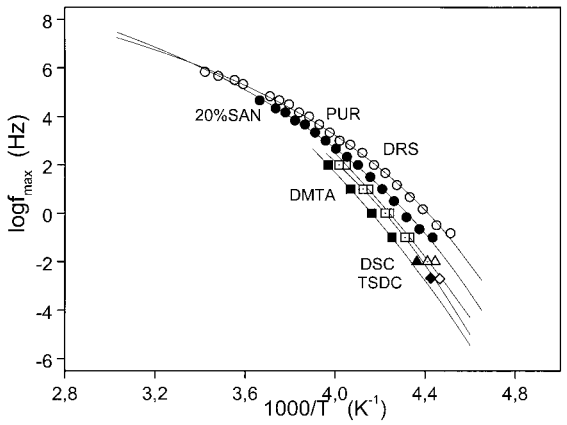

Figure 11 Arrhenius plot of DRS (circles) and DMTA (squares) data for the α relaxation of SS PUR in PUR (open symbols), PUR/10%SAN (dot-inserted symbols), and PUR/20%SAN (solid symbols). Included are DSC (triangles) and TSDC data (wide diamonds).

$$f_{\max} = A \exp\left(-\frac{B}{T - T_0}\right) \quad (5)$$

where A, B, and T_0 (Vogel temperature) are temperature-independent empirical constants (listed in Table I).

For the α relaxation of the PUR SS microphase the mechanical data in Table I give systematically larger values for A and B and lower values for T_0 compared to values of the dielectric data. However, there is some doubt about this comparison, as well as about the systematic variations of A, B, and T_0 (from the mechanical data) with SAN content in Table I, because of the limited frequency range of DMTA measurements and the need for the extrapolations in the VTFH law. In several polymeric systems the Vogel temperature T_0 was found to be in the range of about 50°C lower than T_g.[17,18] With respect to that, and the T_g data in Figure 2, the dielectric fitting parameters in Table I seem to be more reasonable than the mechanical ones. The remark on the limited frequency range of DMTA measurements and the ambiguity about the systematic variations of the VTFH fitting parameters also refer to the data for the α relaxation of the SAN component in Table I.

The dielectric results in Figure 11 and in Table I allow calculation of $T_{g\ \mathrm{diel}}$, defined by $\tau(T_{g\ \mathrm{diel}}) = 100$ s,[24] where $\tau = 1/(2\pi f_{\max})$. This calculation is based on the observation that in several glass-forming systems the dielectric relaxation time becomes in the order of 100 s at the calorimetric T_g.[24,25] The values obtained, −58°C for PUR and −54°C for PUR/20%SAN, are lower than those determined by DSC and TSDC (Fig. 2), although they show the same trend on addition of SAN. For comparison, they were included in Figure 2. In the same figure $T_{g\ \mathrm{mech}}$ values were included, calculated from the mechanical data by the condition $\tau(T_{g\ \mathrm{mech}}) = 100$ s, where τ is the mechanical relaxation time. The $T_{g\ \mathrm{mech}}$ values in Figure 2 are in good agreement with the corresponding DSC and TSDC data.

The dramatic slowing down of $f_{\max}(1/T)$ near T_g suggests that $T_{g\ \mathrm{diel}}$ depends sensitively on the particular choice of τ (or f_{eq}). Sauer et al.[26] suggested using $f_{eq} = 10$ Hz for the transformation of DRS data to T_g values. Already at $f_{eq} = 1$ Hz the DRS data in Figure 11 give $T_{g\ \mathrm{diel}} = -45$°C for PUR and −41°C for PUR/20%SAN, that is, higher than the corresponding DSC and TSDC values (Fig. 2). The comparison of T_g (DSC) and T_α (TSDC) with each other is more straightforward, because both quantities are directly measured. In Figure 2 T_α for each sample is slightly lower than T_g. In general, T_α and T_g have been found to agree rather well with each other for several polymeric systems.[3,4,12,13,22] It should be stressed, however, that even small differences in cooling and heating rate in DSC and TSDC may cause shifts of T_α and T_g to each other because of structural relaxation.

Because the thermodynamic parameters of the dielectric relaxations (Table I) have been calculated, the equivalent frequency of TSDC measurements can now be calculated by means of[11]

$$f_{eq} = \frac{Eb}{2\pi k T_m^2} \quad (6)$$

for the secondary γ and β relaxations and of

$$f_{eq} = \frac{Bb}{2\pi (T_m - T_0)^2} \quad (7)$$

for the primary α relaxation. In these equations b is the heating rate of TSDC measurements and T_m is the TSDC peak temperature. They give $f_{eq} = 2.6$ mHz for γ, 1.6 mHz for β, and 2.0 mHz for α in PUR, and 2.1 mHz for α in PUR/20%SAN. These values are in good agreement with $f_{eq} = 1.6$ mHz, determined by the condition $\tau(T_m) = 100$ s, which was used in Figures 10 and 11.

To discuss the results for the α relaxation of the PUR SS microphase and of SAN in terms of fragility[27] the following modified VTFH equation was fitted to the experimental data in Figures 10 and 11:

$$f_{\max} = A \exp\left(-\frac{DT_0}{T - T_0}\right) \quad (8)$$

where A, D, and T_0 are constants. D is the "strength" parameter, related to the "fragility" parameter m by[27]

$$m = 17 + 580/D \quad (9)$$

The concept of fragility has been much used in recent years to classify glass-forming materials with respect to kinetic and thermodynamic aspects of the glass transition. It has been suggested that the fragility controls a number of properties such as structural state dependence, decoupling phenomena, and nonexponentiality of relaxation.[25,27,28] Fragility has been linked to the density of configurational and vibrational states,

that is, the density of minima in the potential energy hypersurface in configurational space, and the average barrier separating those minima.[27]

The parameters of eq. (8) were equally well fitted with those of eq. (5) to the data in Figures 10 and 11 (the fitting parameters are listed in Table I). The D values of 4.1 and 5.4 for the α relaxation of PUR SS microphase classify PUR and PUR/SAN as fragile systems, in agreement with results obtained with other polyurethane systems.[3,29] The corresponding "mechanical" D values in Table I are larger, indicating a lower fragility. However, there is some doubt about these values and their systematic variation with SAN content because of the limited frequency range of measurements. It was predicted by Angell[25,27] that fragile systems are characterized by large heat capacity change ΔC_p at T_g. In agreement with that prediction, the DSC results give $\Delta C_p = 0.58$ for the normalized ΔC_p of PUR at T_g (normalized to 100% PUR). T_0 in eq. (8) is related to T_g by the relation[25]

$$T_g = T_0(1 + 0.0255D) \tag{10}$$

Equation (10) gives T_g values for the PUR SS microphase (for both the dielectric and the mechanical data in Table I) in the range -89 to -84°C, that is, significantly lower than those determined more directly by DSC, TSDC, DRS (Fig. 2), and DMTA. This is consistent with the T_0 values in Table I, determined by eq. (5), being in the range -136 to -106°C, that is, lower than about T_g -50°C, experimentally observed in many polymeric systems.[17,18]

For the α relaxation of SAN the D values in Table I indicate a fragile system. T_g calculated by eq. (10) is 104°C for PUR/10%SAN and 122°C for PUR/20%SAN, for which the DSC value was 118°C for both samples.

We now discuss the implications of the results obtained by the various techniques on the micromorphology of the samples. Several results provide strong evidence that, on addition of SAN, the degree of microphase separation (DMS) of PUR into HS microdomains and SS microphase increases. In the DSC measurements the increase of DMS is indicated by the overproportional decrease of the specific heat increment ΔC_p at the glass transition of the PUR SS microphase (Fig. 3). This follows from the observation that in segmented polyurethanes ΔC_p increases with increasing phase mixing, the additional contribution arising from the enhanced mobility of HS at the periphery of the HS microdomains.[14] In the DRS and TSDC measurements the increase of DMS on addition of SAN is indicated by the underproportional decrease of the dielectric strength $\Delta\epsilon$ of the α relaxation of the SS microphase (Fig. 3 and comments thereon). From the methodological point of view it is interesting to note here the difference between DSC and dielectric techniques. In addition, for the interfacial MWS TSDC peak both T_{MWS} and $\Delta\epsilon$ were found to increase with increasing SAN content (Fig. 5). It should be stressed that $\Delta\epsilon$ increases, although dc conductivity decreases (Fig. 8). Similar systematic variations in polyurethane systems have been interpreted in terms of increasing DMS.[15,22] Because T_α also changes with composition (Fig. 2), the difference $T_{MWS} - T_\alpha$ should be considered as indicative of DMS rather than T_{MWS}. This difference increases from 34°C in PUR to 38°C in PUR/10%SAN and to 41°C in PUR/20%SAN. Finally, in DMTA measurements (Fig. 9) the increased DMS on addition of SAN is reflected in the strong reinforcing effect observed.[2]

From the methodological point of view, it should be stressed that, only by combining DSC and dielectric results, it unambiguously follows that on addition of SAN the DMS of PUR into HS microdomains and SS microphase increases. In fact, the overproportional decrease of ΔC_p on addition of SAN in Figure 3 could have been attributed to other effects, for example, immobilization of a part of PUR through interaction with SAN, similar to the rigid amorphous phase in semicrystalline polymers.[20] This and similar other interpretations, however, can readily be excluded on the basis of the dielectric results.

The increase of DMS on addition of SAN is attributed to interactions between the SAN copolymer and the HS microdomains. Evidence for that is provided by the shift of the melting endotherm, attributed to softening of the HS microdomains, to lower temperatures on addition of SAN, from 215°C in PUR to 210°C in PUR/20%SAN. Several results indicate that the interaction between the SAN copolymer and the SS microphase is weak. T_g of SAN (118°C) is independent of SAN content. In addition T_g, T_α, and $T_{g\ \mathrm{diel}}$ (Fig. 2) increase only slightly on addition of SAN. The same also holds for the peak temperature of the DMTA loss peak associated with T_g of the PUR SS microphase.[2] The absolute values of the various measures of T_g are different from each other,

although the shifts with SAN content are comparable to each other.

From the methodological point of view the techniques employed can be critically compared to each other, mainly on the basis of the Arrhenius plots in Figures 10 and 11. However, two points should be taken into account. The first refers to the DRS–DMTA comparison. The dielectric complex permittivity ϵ is a compliance, whereas the complex shear modulus G is a modulus. For the same relaxation process, the frequencies of peak maximum (f_{max} in Figs. 10 and 11) are always shifted to higher values for modulus than those for compliance, as a result of the relation between them.[29,30] For a direct comparison, it is possible to convert the data from the one formalism to the other, under the condition that the measurements have been extended to sufficiently low and high frequencies.[29,30] On the other hand, the DRS data in Figures 10 and 11 refer to losses ϵ'', and the mechanical data to loss tangent tan δ. Compared to the peak in shear loss G'', the peak in tan δ is shifted to lower frequencies. Because the shifts for the modulus–compliance and for the losses–loss tangent transformations are in opposite directions to each other and, thus, tend to compensate, it seemed reasonable at this stage not to perform the transformations and, thus, to compare dielectric ϵ'' and shear modulus tan δ peak frequencies with each other, bearing in mind the previously discussed points. It is interesting to mention here that Havriliak Jr. and Havriliak[32] extended a recommendation made by Scaife[33] for the comparison of dielectric data as complex polarizability rather than complex permittivity to the comparison of dielectric and viscoelastic data. The second point to be taken into account, valid for all the techniques, refers to the need to ensure a high reproducibility of the temperature measurements, a truly comparable temperature scale, and measurements on identical samples (e.g., water content).[8,10]

The overall implication from Figure 11 is that the results of DSC, DMTA, and TSDC agree well with each other, whereas the f_{max} values by DRS are shifted, for the same temperature, to up to two decades higher frequencies.

Concerning the comparison between TSDC and DRS data, it has been argued that, although their results compare well for the local secondary relaxations, they are not directly comparable to the α relaxation because of the contribution of free charges to the TSDC α signal.[11] This is partly confirmed by the results in Figures 10 and 11. On the other hand, it has been very often observed that, despite similar values of relaxation times, the TSDC values of activation energy of secondary relaxations in polymers are systematically lower than the DRS values.[34,35] In addition, DRS and TSDC have been found to give very similar results for the α relaxation in other polyurethane systems.[36] For the samples under investigation, the lower values of TSDC equivalent frequencies for the α relaxation of the PUR SS microphase, as compared to those of DRS in Figures 10 and 11, cannot be attributed to the contribution of free charges,[11] because this contribution gives rise to the interfacial MWS peak, which is well separated from the α peak (Fig. 4). In more homogeneous systems the TSDC peak resulting from motion of free charges, "frozen" at temperatures lower than T_g, may overlap with the α peak, so that the resulting peak is shifted to higher temperatures compared to T_g. Kyritsis et al.[37] studied this effect in poly(hydroxyethyl acrylate) hydrogels and described procedures to experimentally resolve the dipolar and the free charge contributions to the composite TSDC peak at T_g.

The equivalent frequency f_{eq} of DSC data in Figures 10 and 11, following eq. (2), is 10 mHz. Equation (3) would give a lower value, f_{eq} = 1.8 mHz, that is, very close to the TSDC data. Hensel et al.[20] compared eqs. (2) and (3) with each other by investigating semicrystalline polymers, in which the mean temperature fluctuation δT is expected to take large values and showed that the product $\alpha\delta T$ in eq. (2) may become significantly larger than the constant value of 15 K in eq. (3). Dobbertin et al.[38] compared DRS and DSC results in a low molecular weight compound by taking f_{eq} = 1 mHz for DSC, corresponding to a heating rate of 10 K/min. Progress in experimental facilities in recent years made possible frequency-dependent heat-capacity measurements, so that a direct comparison in frequency domain with DRS and DMTA is possible. DRS and heat-capacity spectroscopy measurements on phenyl salicylate,[39] which is a low molecular weight glass-former, and on polystyrene[9] showed that the corresponding Arrhenius plots practically coincide in the common frequency range of the two techniques, suggesting that, although the phenomena measured are physically different, both techniques probe at the glass transition the mobility of units of similar size.

DRS and DMTA data in Figure 11 for the α relaxation of the PUR SS microphase, both measured directly in the frequency domain, show that

at each temperature the dielectric process is faster than the mechanical process. This would suggest a larger size for the units responsible for the mechanical processes. As mentioned earlier, however, the mechanical data refer to modulus and tan δ, whereas the dielectric data refer to compliance and ϵ''. For the mechanical data the VTFH fittings give systematically lower values for the Vogel temperature T_0 and higher values for A and B in Table I. Within the fragility scheme, the strength parameter D is larger for the mechanical than for the dielectric α relaxation. However, the frequency range of DMTA measurements is significantly narrower than that of DRS measurements. On the other hand, the DSC and TSDC data in Figure 11 are in better agreement with the DMTA data than with the DRS data. Also for the α relaxation of the SAN component, for which no dielectric data are available, DMTA and DSC data in Figure 10 agree well with each other.

Heat capacity, shear, and dielectric spectroscopy in poly(vinyl acetate) in the region of the glass transition by Beiner et al.[8] show that in the corresponding Arrhenius plot the frequencies of maxima increase in the order dielectric compliance, entropy compliance, and shear modulus. The width of the peaks is also different: the shear loss peak is one decade broader than the other two. Similar measurements in the glass-transition region of polystyrene give, in the Arrhenius plot, approximately similar values for the calorimetric and dielectric data (frequencies of maxima) and higher values for the shear modulus data.[9] Ivanov and Jonas[31] observed that in amorphous poly(aryl-ether-ether-ketone) the results of mechanical and dielectric α relaxation (in the form of mechanical and electrical modulus) were very similar to each other, with respect to both shape of the response and relaxation time, suggesting similarity of the nature of relaxing units examined by both probes. Santagelo and Roland[40] reported that the mechanical and dielectric relaxation times for the α relaxation in 1,4-polyisoprene have identical temperature dependencies, the former being about sixfold smaller. Measurements on poly(vinylethylene) by Colmenero et al.[10] showed similar shape (for the same temperature) and temperature dependence of relaxation times for the mechanical and the dielectric α relaxation and about one decade larger dielectric relaxation times. These results by different authors in various systems suggest that, in general, there are differences in both the temperature (frequency) position and the shape of the α loss peak measured by different techniques. This results from the fact that, for a given system, each technique is sensitive to specific modes of the general, broad frequency spectrum of cooperative motions at the dynamic glass transition.[7,8]

CONCLUSIONS

Microphase separation and molecular mobility in blends of crosslinked polyurethanes (PURs) and styrene–acrylonitrile (SAN) copolymer, prepared by reactive blending with polymer polyols, were investigated by means of differential scanning calorimetry (DSC), thermally stimulated depolarization currents (TSDC) techniques, dielectric relaxation spectroscopy (DRS), and dynamic mechanical thermal analysis (DMTA). The combination of several experimental techniques in wide ranges of frequency and temperature allowed the study of several relaxation mechanisms present in the pure components and in the blends.

Each of the techniques employed provided evidence that the degree of microphase separation (DMS) of PUR into hard-segment (HS) microdomains and soft-segment (SS) microphase increases on addition of SAN. This arises from SAN–HS interactions, whereas SAN–SS interactions are negligibly weak. Two results should be emphasized here. First, the difference $T_\alpha - T_{\mathrm{MWS}}$, where T_α and T_{MWS} are the TSDC peak temperatures of the α relaxation and of the interfacial Maxwell–Wagner–Sillars relaxation, respectively, increases with increasing DMS and seems to be a good measure of that. It should be interesting to check this criterion with that of other polyurethane systems. Second, the normalized specific heat increment ΔC_p at the glass transition of the PUR SS microphase (normalized to the same PUR content) decreases on addition of SAN and the resulting increase of DMS, whereas the normalized dielectric relaxation strength of the associated α relaxation increases. Thus, DSC and DRS are sensitive to different aspects of phase interaction and mixing.

By means of empirical relationships, TSDC, DRS, and DMTA provide, through the investigation of the dynamic glass transition, measures of the glass-transition temperature. For the glass transition of the PUR SS microphase, these show, on addition of SAN and increase of DMS, the same trend as the calorimetric T_g. The absolute values, however, depend sensitively on the partic-

ular choice of the characteristic relaxation time (or equivalent frequency) at T_g.

The various techniques employed to investigate molecular mobility were critically compared to each other on the basis of activation diagrams, particularly for the dynamic glass transition of the PUR SS microphase. Processes characterized, in general, by different time and length scales can be compared to each other on the basis of such diagrams and by introducing equivalent frequencies for the DSC and the TSDC data. The results suggest that for the α relaxation of PUR SS microphase the characteristic time scales at the same temperature are similar for DMTA, DSC, and TSDC and shorter for DRS. In agreement with results obtained with several other systems, the results here point to the fact that, for a given system, each technique is sensitive to specific modes of the general, broad frequency spectrum of cooperative motions at the dynamic glass transition.[7,8]

The concept of fragility has been much used in recent years to classify glass-forming materials with respect to kinetic and thermodynamic aspects of the glass transition and, in addition, fragility has been linked to the density of configurational and vibrational states.[27] The results obtained within this work suggest that, with respect to the dynamic glass transition of both the PUR SS microphase and the SAN component, the PUR/SAN blends are fragile systems.

The authors thank Prof. R. Becker and Dr. E. Mitzner for the preparation of samples, Dr. A. Schoenhals for using his ac equipment, and Dr. E.-H. Carius and Dr. H. Goering for helpful discussions.

REFERENCES

1. Koberstein, J. T.; Galambos, A. F.; Leung, L. M. Macromolecules 1992, 25, 6195.
2. Mitzner, E.; Goering, H.; Becker, R. Die Angewandte Macromolekulare Chemie 1994, 220, 177.
3. Kanapitsas, A.; Pissis, P.; Garcia Estrella, A. Eur Polym J 1999, 35, 923.
4. Kyritsis, A.; Pissis, P.; Grigorieva, O. P.; Sergeeva, L. M.; Brovko, A. A.; Zimich, O. N.; Privalko, E. G.; Shtompel, V. I.; Privalko, V. P. J Appl Polym Sci 1999, 73, 385.
5. Campbell, D.; White, J. R. Polymer Characterization; Chapman & Hall: London, 1989.
6. Spells, S. J., Ed. Characterization of Solid Polymers; Chapman & Hall: London, 1994.
7. Donth, E. Relaxation and Thermodynamics in Polymers: Glass Transition; Akademie: Berlin, 1992.
8. Beiner, M.; Korus, J.; Lockwenz, H.; Schroeter, K.; Donth, E. Macromolecules 1996, 29, 5183.
9. Weyer, S.; Hensel, A.; Korus, J.; Donth, E.; Shick, C. Thermochim Acta 1997, 251, 304.
10. Colmenero, J.; Alegria, A.; Santagelo, P. G.; Ngai, K. L.; Roland, C. M. Macromolecules 1994, 27, 407.
11. Boersma, A.; van Turnhout, J.; Wuebbenhorst, M. Macromolecules 1998, 31, 7453.
12. van Turnhout, J. in Electrets, Topics in Applied Physics, Vol. 33; Sessler, G. M., Ed.; Springer: Berlin, 1980, Chapter 3.
13. Pissis, P.; Anagnostopoulou-Konsta, A.; Apekis, L.; Daoukaki-Diamanti, D.; Christodoulides, C. J Non-Cryst Solids 1991, 1174, 131.
14. Savelyev, Y. V.; Akhranovich, E. R.; Grekov, A. P.; Privalko, E. G.; Korskanov, V. V.; Shtompel, V. I.; Privalko, V. P.; Pissis, P.; Kanapitsas, A. Polymer 1998, 39, 3425.
15. Kanapitsas, A.; Pissis, P.; Gomez Ribelles, J. L.; Monleon Pradas, M.; Privalko, E. G.; Privalko, V. P. J Appl Polym Sci 1999, 71, 1209.
16. Pissis, P.; Kanapitsas, A.; Savelyev, Y. V.; Akhranovich, E. R.; Privalko, E. G.; Privalko, V. P. Polymer 1998, 39, 3431.
17. Hedvig, P. Dielectric Spectroscopy of Polymers; Adam Hilger: Bristol, 1997.
18. Mc Crum, N. G.; Read, B. E.; Williams, G. Anelastic and Dielectric Effects in Polymeric Solids; Wiley: New York, 1967.
19. Runt, J. P.; Fitzgerald, J. J. Dielectric Spectroscopy of Polymeric Materials; American Chemical Society: Washington, DC, 1997.
20. Hensel, A.; Dobbertin, J.; Schawe, E. K.; Boller, A.; Schick, C. J Therm Anal 1996, 46, 935.
21. Heinrich, W.; Stoll, B. Prog Colloid Polym Sci 1998, 78, 37.
22. Georgoussis, G.; Kanapitsas, A.; Pissis, P.; Savelyev, Y. V.; Veselov, V. Y.; Privalko, E. G. Eur Polym J to appear.
23. Jaeckle, J. Rep Prog Phys 1986, 49, 171.
24. Ngai, K. L.; Roland, C. M. Macromolecules 1993, 26, 6824.
25. Angell, C. A. Annu Rev Phys Chem 1992, 43, 693.
26. Sauer, B. B.; Avakian, P.; Flexman, E. A.; Keating, M.; Hsiao, B. S.; Verma, R. K. J Polym Sci Part B Polym Phys 1997, 35, 2121.
27. Angell, C. A. J Non-Cryst Solids 1991, 13, 131.
28. Boehmer, R.; Ngai, K. L.; Angell, C. A.; Plazek, D. J. J Chem Phys 1993, 99, 4201.
29. Kanapitsas, A.; Pissis, P.; Karabanova, L.; Sergeeva, L.; Apekis, L. Polym Gels Networks 1998, 6, 83.
30. Tabellout, M.; Baillif, P.-Y.; Randrianantoandro, H.; Litzinger, F.; Emery, J. R. Phys Rev B 1995, 51, 12295.
31. Ivanov, D. A.; Jonas, A. M. Polymer 1998, 39, 3577.
32. Havriliak, S., Jr.; Havriliak, S. J. J Mol Liq 1998, 69, 305.

33. Scaife, B. K. P. Proc Phys Soc London 1963, 81, 124.
34. Vanderschueren, J.; Linkens, A. J Electrostat 1977, 3, 155.
35. Kyritsis, A.; Pissis, P. J Polym Sci Part B Polym Phys 1997, 35, 1545.
36. Georgoussis, G.; Kyritsis, A.; Pissis, P.; Savelyev, Y. V.; Akhranovich, E. R.; Privalko, E. G.; Privalko, V. P. Eur Polym J 1999, 35, 2007.
37. Kyritsis, A.; Pissis, P.; Gomez Ribelles, J. L.; Monleon Pradas, M. J Polym Sci Part B Polym Phys 1994, 32, 101.
38. Dobbertin, J.; Hannemann, J.; Schick, C.; Poetter, M.; Dehne, H. J Chem Phys 1998, 108, 9062.
39. Dixon, P. K. Phys Rev B 1990, 42, 8179.
40. Santangelo, P. G.; Roland, C. M. Macromolecules 1998, 31, 3715.